

Electronic structure and isomer shifts of Sn halides

Joice Terra and Diana Guenzburger

*Centro Brasileiro de Pesquisas Físicas (CBPF), Conselho Nacional de Desenvolvimento Científico e Tecnológico (CNPq),
Rua Dr. Xavier Sigaud, 150, 22290, Rio de Janeiro, Rio de Janeiro, Brazil*

(Received 2 May 1988; revised manuscript received 29 August 1988)

The all-electron first-principles discrete variational method was employed to study the electronic structure of SnF_4 , SnCl_4 , SnBr_4 , and SnI_4 . Values of the electronic density at the Sn nucleus were derived and related to ^{119}Sn isomer shifts to obtain the nuclear constant $\Delta\langle r^2 \rangle$. Differences in values of $\rho(0)$ are discussed in terms of the chemical bonding between Sn and halogen atoms.

I. INTRODUCTION

The isomer shift, δ , as measured by Mössbauer spectroscopy, depends on both a nuclear factor and an electronic factor.¹ The latter, $\Delta\rho(0)$, is the difference between the electronic density at the nucleus in the probe atom in two different environments and reflects the difference in the chemical interactions of this atom. For this reason, the isomer shift can give important information about the electronic structure and chemical bonding in compounds and alloys, and a wide variety of applications have been made in chemistry and solid-state physics. However, the qualitative and quantitative interpretation of this information requires knowledge of the nuclear factor, which is the relative variation of the nuclear radius $\Delta R/R$ in the Mössbauer transition.

In the case of the most widely studied Mössbauer probe, ^{57}Fe , the nuclear constant $\Delta R/R$ has already been reasonably well established through a large number of experimental and theoretical efforts.¹⁻³ For the less-studied Mössbauer isotope ^{119}Sn , a number of determinations of $\Delta R/R$ have been made. So far, the majority of the proposed values for the $\Delta R/R$ have been obtained in two ways. It may be obtained either by combining the difference in isomer shift for two distinct chemical states of Sn with the calculated value of the charge density at the nucleus for each of the states,⁴⁻¹⁷ or it can be derived by combining a change in isomer shift with an estimate, by some other technique (as for example internal conversion) of the corresponding change in the electron density at the nucleus and a calculation of the electron density for one state of Sn.¹⁸⁻²¹

These earlier calculations of $\rho(0)$ have been made considering the Sn atom as free,⁴⁻²¹ mainly due to the fact that Sn is a considerably larger atom than Fe, thus constituting a bigger challenge for electronic-structure calculations. However, Mössbauer experiments on matrix-isolated Sn have shown that even rare-gas matrix effects on $\rho(0)$ might be of the order of $\sim 5\%$.¹⁵ Accordingly, the extensive contradiction between the values of $\Delta R/R$ estimated with the use of atomic wave functions may be ascribed to the neglect of the ligands, which is unsuitable because no proper account is taken of the neighborhood effects on the probe atom.

In this work we present a determination of $\Delta R/R$ for

^{119}Sn by means of first-principles all-electrons self-consistent electronic-structure calculations on four compounds of Sn, namely SnF_4 , SnCl_4 , SnBr_4 , and SnI_4 , employing the discrete variational (DV) linear combination of atomic orbitals (LCAO) molecular-orbital method^{22,23} in the local-density approximation. Local-density methods have been employed to study isomer shifts,²⁴ and the DV method was used to investigate isomer shifts in inorganic compounds,²⁵ as well as metals and alloys.²⁶ The choice of these compounds was based on the fact that they are solids with a well-defined crystallography, besides spanning a wide range of values of δ . Values of the electronic density at the Sn nucleus were derived for these compounds, and were combined with the experimental δ values to obtain the nuclear factor. Differences in $\rho(0)$ obtained are discussed in the light of the different factors related to the chemical bonds.

A few attempts to calculate $\rho(0)$ for Sn compounds and Sn metal have been reported very recently in the literature.²⁷⁻³⁰ Here we analyze briefly the differences and similarities between our method and those of these authors, and compare the results.

This paper is organized as follows. In Sec. II we describe the main features of the theoretical method and calculation procedure. In Sec. III we present and discuss the results obtained. In Sec. IV we summarize our main conclusions.

II. THEORETICAL METHOD

A. Discrete variational method

We employed the discrete variational method (DVM) in the local-density approximation, as has been described in detail elsewhere,^{22,23,31} to perform electronic-structure calculations of clusters representing the solids. The fundamental problem is to solve the set of one-electron equations

$$(H - \epsilon_i)\psi_i(\mathbf{r}) = 0, \quad (1)$$

where the one-electron Hamiltonian is given (in Hartrees) by

$$H = -\frac{1}{2}\nabla^2 + V_{\text{Coul}}(\rho) + V_{x\alpha}(\rho), \quad (2)$$

where the local exchange potential $V_{x\alpha}$ is^{32,33}

$$V_{x\alpha}(\rho) = -3\alpha \left[\frac{3}{8\pi} \rho(\mathbf{r}) \right]^{1/3} \quad (3)$$

with $\alpha = \frac{2}{3}$. The Coulomb potential V_{Coul} includes nuclear and electronic contributions and the electronic density $\rho(\mathbf{r})$ at point \mathbf{r} is taken as a sum over the molecular orbitals ψ_i with occupation n_i

$$\rho(\mathbf{r}) = \sum_i n_i |\psi_i(\mathbf{r})|^2. \quad (4)$$

The one-electron molecular wave functions are expanded on a basis of symmetrized numerical atomic orbitals χ_j^s (LCAO approximation)

$$\psi_i(\mathbf{r}) = \sum_j c_j^i \chi_j^s(\mathbf{r}). \quad (5)$$

The coefficients that define the molecular orbitals $\psi_i(\mathbf{r})$ and their one-electron energies ϵ_i are found by solving the secular equations

$$([H] - [E][S])[C] = 0, \quad (6)$$

where the matrix elements are numerical integrals on a three-dimensional grid. The integrations are performed in three dimensions with the pseudorandom diophantine method.²² For the calculation of hyperfine interactions, however, additional caution is required in the numerical procedures at the core region of the probe atom, where precision of the matrix elements is difficult to achieve due to the large oscillations of the wave functions. For this reason, a special integration scheme was used inside a sphere containing the core electrons of the probe atom, involving a systematic polynomial integration in three dimensions.³¹

An approximation to $\rho(\mathbf{r})$ is employed to define the Hamiltonian in Eq. (2).²³ A Mulliken-type population analysis is performed for the atoms in the cluster and the charge density is approximately defined as

$$\rho(\mathbf{r}) \cong \sum_{v,n,l} f_{nl}^v |R_{nl}(r_v)|^2, \quad (7)$$

where $R_{nl}(r_v)$ is the radial part of atomic orbital $\chi_v(\mathbf{r}) = R_{nl}(r_v) Y_l^m(\hat{\mathbf{r}}_v)$ centered on site v , and f_{nl}^v is the Mulliken-type population of this orbital. Iterations are made until the populations achieve self-consistency. All electrons are included in the calculations, and the core is completely relaxed.

In the DV method, the crystal is simulated by an embedding scheme, where we considered numerical atomic potentials at a number of sites surrounding the cluster. Since the chemical environment of the solid is thus considered, the main question is the definition of the clusters, which must be chosen as the most representative of the crystal, that is to say, they must provide an adequate representation of the neighborhood felt by the tin atom. For SnCl_4 , SnBr_4 , and SnI_4 , we considered the tetrahedral clusters present in the crystals.^{34,35} Mössbauer spectroscopy measurements on the Ar matrix-isolated molecules SnX_4 ($X = \text{Cl}, \text{Br}, \text{I}$) show that, within the experimental error, the isomer shifts of Sn in these species are identical to the crystals.³⁶ This result

indicates that our choice of clusters in these cases is very reasonable. In the solids, the tetrahedral coordination around the Sn is slightly distorted,^{34,35} however, this distortion was not considered in our calculations, and T_d symmetry was adopted. On the other hand, the same experiments on matrix-isolated tin^{4+} fluoride³⁶ showed a marked difference in the Mössbauer parameters, as compared to the crystalline solid. Indeed, this solid has a layered structure,³⁷ which results in a strong tetragonal distortion of the octahedral coordination of the six fluorine atoms surrounding the Sn, the axial Sn—F interatomic distances being shorter than the equatorial distances. It is this distortion which gives rise to the observed quadrupole splitting in crystalline SnF_4 .³⁸ In the tetragonal (D_{4h}) cluster $(\text{SnF}_6)^x$ considered in our calculation, this distortion was taken into account, with interatomic distances as in the crystal. The charge ($-x$) of the cluster was determined self-consistently, as described later. In Fig. 1 we show the two types of clusters and in Table I are given the interatomic distances.

B. Mössbauer isomer shift

The isomer shift δ , as defined in a Mössbauer spectroscopy measurement, formally can be written as^{1,38}

$$\delta = \alpha \Delta\rho_e(0) \quad (8)$$

with

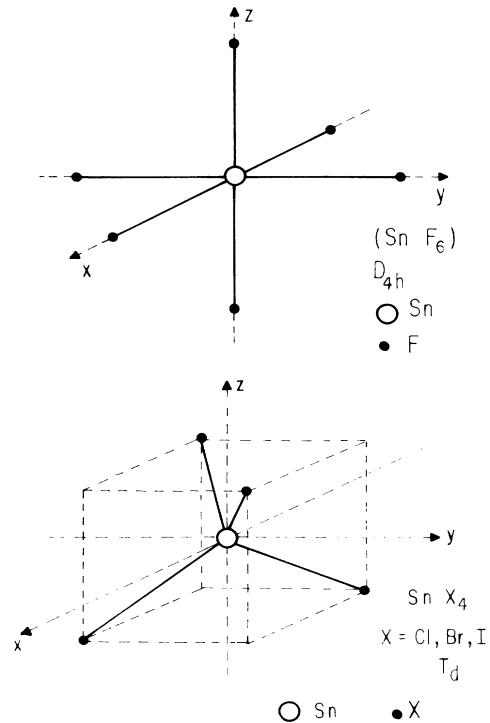


FIG. 1. Clusters representing Sn halide crystals.

TABLE I. Crystallographic data for Sn halides (see Refs. 34, 35, and 37).

	(SnF ₆) ^{x-}	SnCl ₄	SnBr ₄	SnI ₄
Crystallographic structure	Tetragonal	Monoclinic	Monoclinic	Cubic
Sn—X distance (Å)	2.02(eq.) 1.88(ax.)	2.26 ^a	2.46 ^a	2.69 ^a
X-Sn-X angle (deg)		102.25	109.25	
Lattice parameters (Å)	4.04 4.04 7.93	9.80 6.75 9.98	10.59 7.10 10.66	12.26 12.26 12.26

^aAverage distance.

$$\alpha = \frac{2}{3}\pi Ze^2 \Delta \langle r^2 \rangle S'(Z)$$

or (9)

$$\alpha = \frac{4}{5}\pi Ze^2 R^2 (\Delta R / R) S'(Z)$$

and

$$\Delta \rho_e(0) = \sum_i n_i |\psi_i(0)|_A^2 - \sum_j n_j |\psi_j(0)|_s^2, \quad (10)$$

where $\Delta \langle r^2 \rangle$ is the difference in the mean-square nuclear radius, whereas $\Delta R / R$ is the change in the nuclear charge radius for a uniform charge distribution of $R = 1.2 A^{1/3}$ fm, between the excited and ground states in the Mössbauer nuclear transition (23.8 keV for ¹¹⁹Sn). The chemical term is the difference between the electron charge density at the nuclear site related to the absorber A and the source S , the summations being over the molecular orbitals ψ_i occupied by n_i electrons [see Eq. (4)]; $S'(z)$ is the correction factor [2.306 for ¹¹⁹Sn (Ref. 6)] if relativistic effects are not taken into account in the calculation of the wave functions.

We have derived the nuclear factors $\Delta \langle r^2 \rangle$ (or $\Delta R / R$) in Eq. (9) by combining experimental measurements of δ in the four crystals studied with the corresponding calculated values of $\Delta \rho_e(0)$, as in Eq. (10). The correction for relativistic effects employed can be considered suitable. Indeed, it has been demonstrated that *differences* in $\Delta \rho_e(0)$ for ions in different oxidation states are well described by nonrelativistic charge density differences multiplied by the linear factor $S'(Z)$.³⁹ Since our study is essentially comparative, the same reasoning applies here, and the errors introduced by the use of nonrelativistic wave functions and a constant $S'(Z)$ are not very significant. Only the molecular orbitals belonging to the totally symmetric representation will have finite probability at the origin.

III. RESULTS AND DISCUSSION

A. Some details of the calculations

As described in Sec. II, our calculations involve an expansion of the one-electron molecular functions on a basis of numerical self-consistent local-density atomic or-

bitals. As this basis is necessarily incomplete, it must be chosen carefully. Winkler *et al.*²⁷ pointed out to be fact that truncated basis sets in LCAO methods may constitute a severe limitation to realistic estimates of isomer shifts, due to lack of flexibility. However, in the present calculations this limitation was largely bypassed by the following procedure: at the end of each convergence of the self-consistent potential, a Mulliken-type population analysis is performed, and the populations obtained used to define atomic charges and configurations for the Sn and halogen atoms. For these configurations, new self-consistent atomic calculations are performed to obtain new atomic orbitals for the basis. This procedure is repeated until the configuration of the basis atomic orbitals is approximately the same as that of the "atoms" in the cluster. This adaptation of the atomic wave functions to the actual situation in the compound compensates to a large extent the limitation on the number of terms in the LCAO expansion.

For the Sn atom, the virtual orbitals 6s and 6p were added to the basis to augment the variational freedom. To further increase the quality of the valence basis functions, a potential well was included in the atomic potential (in the atomic calculations) so as to somewhat contract the diffuse exterior orbitals, creating functions more consistent with the actual situation in the solid. This well was defined with the same characteristics for Sn in all four clusters, so as not to impair the comparison among the compounds, and it was chosen carefully so as not to alter significantly the shape of the valence orbitals of the atom, a feature found to be important for a good description of the isomer shifts.

No empty orbitals were included for the halogen atoms Cl, Br, and I, and no well was considered necessary. In fact, test calculations using potential wells on the halogen atoms showed that even small distortions of the valence functions of the large atoms (Br and I) may affect critically the value of $\rho(0)$ at the Sn site, due to the contribution to $\rho(0)$ of the neighbor atoms diffuse functions. For the F atom, which acquired a much larger negative charge during the self-consistent process, as compared to the other three halogens, a more rigid potential well was necessary, to achieve convergence and to obtain more contracted valence functions, thus getting more meaningful results. This feature has been noticed before in DVM

calculations for the ionic compounds CaF_2 , SrF_2 , and BaF_2 .⁴⁰ Part of the reason for this characteristic is that large negative charges lead to very diffuse orbitals, and for these the Mulliken populations poorly represent the atomic charges, and consequently, so do the self-consistent cluster potentials based on them [see Eq. (7)].

As described in Sec. II, an embedding scheme was employed, with the inclusion of several shells of numerical atomic densities centered on the crystal sites exterior to the cluster, thus creating an embedding potential. Again, the atomic densities for the outer atoms were obtained by atomic local-density self-consistent calculations, for the same configurations as in the cluster. It was gratifying to observe that all three sets of atomic configurations (cluster, basis, and exterior atoms) do, indeed, converge to the same point, making us confident that a consistent picture was obtained for the electronic structure of the crystals.

As mentioned in Sec. II, all electrons were included in the calculations. Although the differences in $\rho(0)$ for the 1s, 2s, and 3s orbitals of Sn in the different clusters may be considered negligible, the inclusion of all orbitals in the self-consistent calculations assures that all effects of core relaxation due to rearrangement of the valence electrons are properly taken into account.

B. Electronic structure

In Table II are given the self-consistent Mulliken populations and the charges for all four clusters investigated. The charge of -1.5 on the fluorine cluster was obtained self-consistently, in order that the charges on the atoms approximately obey the stoichiometry of the compound SnF_4 . At the end of each convergence, the total number of electrons was modified to satisfy the stoichiometry, using the charge on Sn as a guide.

The positive charge on Sn decreases from F to I, as expected from the increase in covalency of the Sn—X bond. There is a marked difference between the charge on Sn in the $\text{SnF}_6^{1.5-}$ cluster and the Sn charge on the other clusters. This is consistent with the marked difference in

electronegativity between F and the other halogens. But even for this most ionic case, the charges are very far from the formal $+4$ for Sn and -1 for F. The decrease of the positive charge on Sn along the series corresponds to an increase in the occupation of the valence orbitals 5s and 5p. In the case of SnI_4 , the 6p orbital was also significantly populated. In the case of $(\text{SnF}_6)^{1.5-}$, there is a marked depletion of the 5s and 5p orbitals, corresponding to a charge transfer from the Sn atom to the F atoms, which is more pronounced for the equatorial fluorines.

In Fig. 2 are shown the higher-energy one-electron energy levels of the clusters [eigenvalues ϵ_i of Eq. (1)], where the dashed line means the first empty level. For $(\text{SnF}_6)^{1.5-}$, the lower-energy set, constituted by molecular orbitals $8a_{1g}$ to $2b_{2g}$, forms the 4d band of Sn. The next group formed by $9a_{1g}$, $5a_{2u}$, and $5e_u$ is predominantly of F(2s) character, both axial and equatorial. The orbitals $4b_{1g}$, $10a_{1g}$, and, in particular, $11a_{1g}$ are the ones that show more admixture between the Sn and F orbitals, with the Sn 4d orbitals participating in the first two forming bonds with the F 2s, and the Sn 5s orbital participating in the latter. Bonding between the Sn 5p orbital and F is seen in the next orbitals $6e_u$ and $6a_{2u}$. Finally, the set from $5b_{1g}$ to the last-occupied orbital $4e_g$ forms the 2p band of fluorine, having negligible contribution of the Sn orbitals. The overall characteristic of the electronic structure of $(\text{SnF}_6)^{1.5-}$ is of a predominantly ionic compound, with little mixture between the Sn and F orbitals.

The situation is markedly different for the other three halides, where covalent admixture of the Sn and halogen atoms is considerably more pronounced. This feature forms the basis of the interpretation of the isomer shifts, as will be discussed in a later section.

The lower-energy set of orbitals for SnCl_4 , as depicted in Fig. 2, is formed by $9t_2$ and $3e$, which are constituted primarily of 4d functions of Sn. The $8a_1$ and $10t_2$ orbitals, which are next in energy, show some admixture with the Sn 5s ($8a_1$), 4d and 5p ($10t_2$) orbitals, but are predominantly of Cl 3s character. $9a_1$ shows a large degree of mixture between Sn 5s and Cl 3s, and in $11t_2$ the mixture

TABLE II. Charges and Mulliken populations for the Sn clusters.

		$(\text{SnF}_6)^{1.5-}$	SnCl_4	SnBr_4	SnI_4
Sn	4s	1.998	1.993	1.994	1.997
	4p	5.997	5.996	5.996	5.997
	4d	9.992	9.994	9.995	9.996
	5s	0.578	1.141	1.300	1.506
	5p	0.470	1.077	1.305	1.568
	6s	0.004	0.015	0.016	0.019
	6p	0.049	0.050	0.070	0.238
	Charge	+2.909	+1.730	+1.319	+0.676
Halogen	2s(eq.)	1.976	2p 5.999	3p 5.999	4s 1.998
	2p(eq.)	5.804	3s 1.970	3d 9.999	4p 5.999
	2s(ax.)	1.975	3p 5.463	4s 1.969	4d 9.999
	2p(ax.)	5.668		4p 5.361	5s 1.959
					5p 5.213
	Charge	-0.780(eq.) -0.644(ax.)	-0.432	-0.329	-0.169

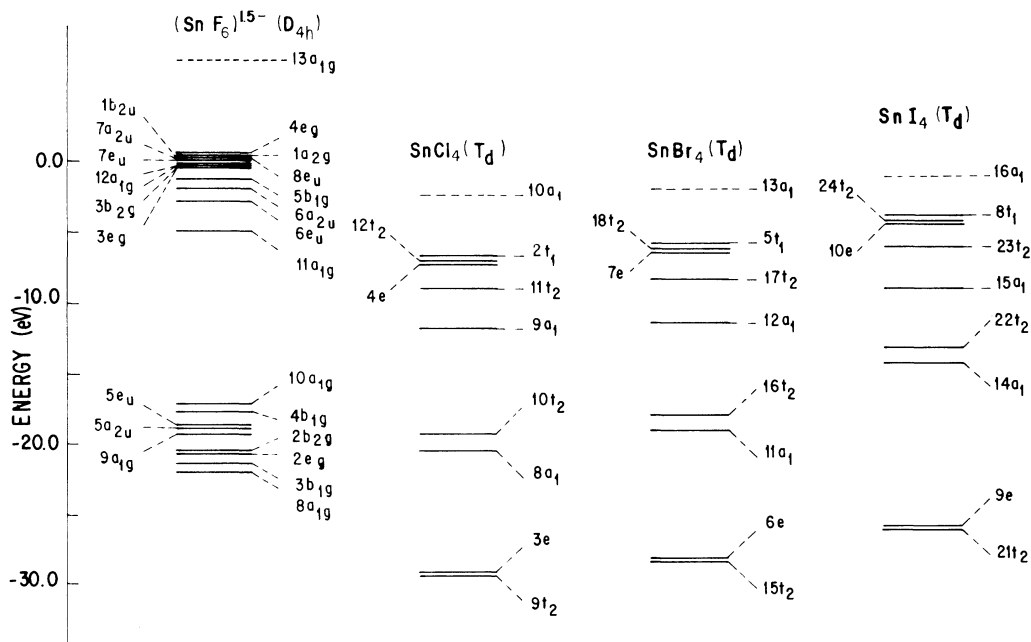


FIG. 2. Valence one-electron energy levels scheme for Sn clusters.

between Sn $5p$, Cl $3s$, and Cl $3p$ is also large. The last three occupied levels are essentially of Cl $3p$ character.

The characteristics of the electronic structure of SnCl_4 are essentially repeated in SnBr_4 and SnI_4 . For those two clusters, the first set of levels ($15t_2$ and $6e$ for SnBr_4 and $21t_2$ and $9e$ for SnI_4) are of Sn $4d$ character. The next four orbitals ($11a_1$, $16t_2$, $12a_1$, and $17t_2$ for SnBr_4 and $14a_1$, $22t_2$, $15a_1$, and $23t_2$ for SnI_4) are of covalent nature, presenting considerable mixture of Sn $5s$, $4d$, and $5p$ orbitals with the valence orbitals of the halogen atom. Finally, the highest-occupied three orbitals of e , t_2 , and t_1 symmetry are essentially constituted of the valence p orbitals of the halogen.

Overall, covalent admixture between Sn and halogen orbitals increases along the series. One may observe also that the energies of the valence orbitals of the clusters of T_d symmetry increase with increasing atomic number of the halogen.

C. Isomer shifts

Analyzing the contributions to $\rho(0)$ of the individual orbitals of appropriate symmetry, it is found that the increase in $\rho(0)$ along the series of halides is related to an increase in the participation of the Sn $5s$ orbital in the valence Molecular Orbitals of a_1 symmetry (or a_{1g} , in the fluoride case). This is consistent with the increase in covalent character from SnF_4 to SnI_4 . In Table III are given the individual contributions for $(\text{SnF}_6)^{x-}$, as an example. For each of the orbitals considered are also shown the energy and the electronic distribution in terms of Mulliken populations. Most of the contribution to $\rho(0)$ comes from the $11a_{1g}$ orbital, with $\sim 24\%$ Sn $5s$ character. For the other halides, the last occupied orbital of a_1 symmetry is the one which contributes mostly to $\rho(0)$, with increasing Sn $5s$ character along the series (40% for SnCl_4 , 46% for SnBr_4 , and 49% for SnI_4).

TABLE III. Energy, charge distribution, and $\rho(0)$ of molecular orbitals of symmetry a_{1g} for $(\text{SnF}_6)^{1.5-}$.

Orbital	Energy (eV)	Charge distribution (% of one electron)	$\rho(0)$ (units of a_0^{-3})
$7a_{1g}$	-117.06	$\sim 100\%$ Sn ($4s$)	314.37
$8a_{1g}$	-22.26	74.7 Sn ($4d_{z^2}$), 2.0 F ($2s_{\text{eq}}$), 21.8 F ($2s_{\text{ax}}$), 1.3 F ($2p_{\text{ax}}$)	0.12
$9a_{1g}$	-19.54	2.2 Sn ($5s$), 1.1 Sn ($4d_{z^2}$), 76.9 F ($2s_{\text{eq}}$), 19.2 F ($2s_{\text{ax}}$)	1.89
$10a_{1g}$	-17.44	26.3 Sn ($4d_{z^2}$), 20.6 F ($2s_{\text{eq}}$), 52.6 F ($2s_{\text{ax}}$)	0.15
$11a_{1g}$	-5.18	23.9 Sn ($5s$), 3.9 F ($2s_{\text{eq}}$), 51.4 F ($2p_{\text{eq}}$), 5.6 F ($2s_{\text{ax}}$), 14.4 F ($2p_{\text{ax}}$)	15.39
$12a_{1g}$	-0.57	4.4 Sn ($4d_{z^2}$), 30.3 F ($2p_{\text{eq}}$), 64.1 F ($2p_{\text{ax}}$)	0.62

Another important feature to be noticed in Table III is the admixture of the $4d_{z^2}$ orbital of Sn in the valence orbitals which contribute to $\rho(0)$, which is possible since the Sn $4d_{z^2}$ orbital transforms as a_{1g} in D_{4h} symmetry. This shows that molecular orbitals calculations of $\rho(0)$ of Sn compounds that treat the $4d_{z^2}$ orbital as "core" are inappropriate.

The total values of $\rho(0)$ are correlated to the experimental isomer shifts in Fig. 3. As both $\rho(0)$ and the measured values of δ increase along the series, we obtain a positive calibration constant in Eq. (8), with the following values for the nuclear constants of ^{119}Sn

$$\Delta\langle r^2 \rangle = +9.21 \times 10^{-3} \text{ fm}^2$$

or

$$\Delta R/R = +2.20 \times 10^{-4} \text{ with } R = 1.2 \times A^{1/3} \text{ fm} .$$

Due mainly to basis functions dependence, we estimate crudely an error of approximately $\pm 10\%$ for these values.

The considerable distance between the point for $(\text{SnF}_6)^{1-}$ from the other halides is consistent with the much more accentuated ionic character of the fluoride.

It is customary in the literature to describe the causes of differences in $\rho(0)$ in different compounds as due mainly to two effects, identified as "potential distortion" and "overlap distortion," both concepts deriving from atomic models. The former is associated to changes in $\rho(0)$ due to changes in the potential around the Mössbauer atom, and the latter is related to orthogonality effects between the core orbitals and valence orbitals on neighbor atoms. In our calculations, these effects are all taken into account simultaneously and in a self-consistent manner. In particular, the inclusion of all core electrons in the calculation is important to include "overlap-distortion" effects in an appropriate manner.

A large number of earlier attempts to obtain $\Delta R/R$ for ^{119}Sn were made employing crude atomic models, resulting in values of $\Delta R/R$ ranging from -2.5 to $+3.6 \times 10^{-4}$.²¹ The recently reported first-principles cal-

culations of Winkler *et al.*²⁷ also resulted in a very good correlation between $\rho(0)$ and δ for Sn^{IV} halides. However, the LCAO Gaussian expansion method employed by the authors had the rather severe limitation of the pseudopotential approximation for the core, and poor flexibility of the basis set, which the authors attempted to circumvent in a rather "ad hoc" manner. The multiple scattering method, which was also employed, does not have these limitations, although its use is restricted to compact clusters; however, the muffin-tin approximation to the cluster potential adopted in this method is rather poor, and it has been shown⁴¹ that calculated values of $\rho(0)$ are extremely sensitive to the muffin-tin radii chosen. Nevertheless, the values of $\Delta R/R$ derived by these authors do not differ very much from our value (2.00×10^{-4} and 1.8×10^{-4} with the pseudopotential LCAO method, and 1.92×10^{-4} with the multiple scattering). In contrast, other very recent attempts to derive $\Delta R/R$ for ^{119}Sn resulted in values which are considerably smaller than ours. The semiempirical molecular orbital calculations performed by Grodzicki *et al.*²⁸ on a large number of Sn^{II} and Sn^{IV} compounds give $\Delta R/R = 1.61 \times 10^{-4}$. The valence-only linear muffin-tin orbitals (LMTO) band-structure calculations of Svane and Antoncik²⁹ for Sn metal and Sn compounds give $\Delta R/R = 1.34 \times 10^{-4}$. Finally, Chow *et al.*³⁰ performed non-self-consistent relativistic augmented plane wave (RAPW) band calculations for metallic Sn at several values of the lattice constant to relate to isomer shift values at different pressures and obtained $\Delta R/R = 1.35 \times 10^{-4}$. We propose tentatively as the main cause of the difference between these values and ours the poor treatment given to the core in these calculations. In particular, as pointed out in Sec. III C, the $4d$ orbital of Sn, often treated as core, should be kept in the variational space.

IV. CONCLUSIONS

We have performed first-principles all-electron electronic-structure calculations for Sn^{IV} halides and derived a value of 2.20×10^{-4} for the nuclear parameter $\Delta R/R$ of ^{119}Sn . A good correlation between $\rho(0)$ and δ was obtained with the DV method. The use of configuration-adapted numerical atomic orbitals in the LCAO basis, crystal embedding, and inclusion of core electrons are a definite improvement over conventional LCAO methods. However, the problem of limited basis sets still remains, and results are consequently somewhat sensitive to the basis functions. The use of numerical self-consistent atomic basis functions optimized to the physical problem at hand offers very interesting possibilities to be explored further.

ACKNOWLEDGMENTS

This work was supported by the Conselho Nacional de Desenvolvimento Científico e Tecnológico (CNPq) and by the National Science Foundation Grant No. INT 83-12863.

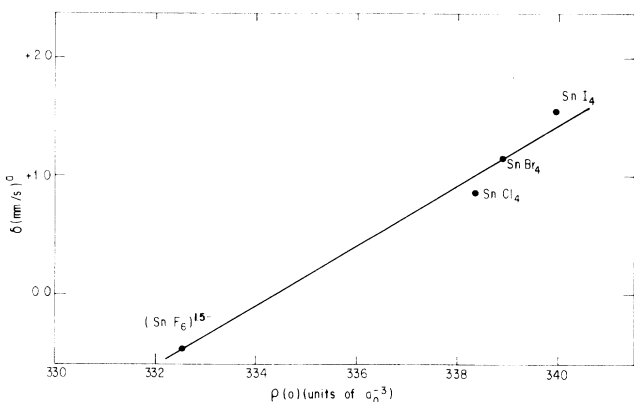


FIG. 3. Isomer shift $\delta\rho(0)$ correlation for Sn halides. Experimental values from Ref. 38. Related to SnO_2 .

- ¹See, for example, *Mössbauer Isomer Shifts*, edited by G. K. Shenoy and F. E. Wagner (North-Holland, Amsterdam, 1978).
- ²D. Guenzburger, D. M. Esquivel, and J. Danon, *Phys. Rev. B* **18**, 4561 (1978).
- ³W. C. Neuwpoort, D. Post, and P. Th. van Duijnen, *Phys. Rev. B* **17**, 91 (1978).
- ⁴A. J. Boyle, St. P. Bunbury, and C. Edwards, *Proc. Phys. Soc. London* **79**, 416 (1962).
- ⁵V. I. Goldanskii, G. M. Gorodinskii, S. V. Karyagin, L. A. Koritko, L. M. Karizhanskii, E. F. Makarov, I. P. Suzdalev, and V. V. Khrapov, *Proc. Acad. Sci. USSR* **147**, 766 (1962).
- ⁶D. A. Shirley, *Rev. Mod. Phys.* **36**, 339 (1964).
- ⁷M. Cordey-Hayes, *J. Inorg. Nucl. Chem.* **26**, 915 (1964).
- ⁸I. B. Bersuker, V. I. Goldanskii, and E. F. Makarov, *Zh. Eksp. Teor. Fiz.* **49**, 699 (1966) [*Sov. Phys.—JETP* **22**, 485 (1966)].
- ⁹S. L. Ruby, G. M. Kalvius, G. B. Beard, and R. E. Snyder, *Phys. Rev.* **159**, 239 (1967).
- ¹⁰J. K. Lees and P. A. Flinn, *J. Chem. Phys.* **48**, 882 (1968).
- ¹¹N. N. Greenwood, P. G. Perkins, and D. H. Wall, *Phys. Lett.* **28A**, 339 (1968).
- ¹²J. DeVooght, P. M. Gielen, and S. Lejeune, *J. Organomet. Chem.* **21**, 333 (1970).
- ¹³H. Micklitz and P. H. Barret, *Phys. Rev. B* **5**, 1704 (1972).
- ¹⁴E. Antoncik, *Phys. Status Solidi B* **79**, 605 (1977).
- ¹⁵H. Micklitz, *Hyperfine Interact.* **3**, 135 (1977).
- ¹⁶E. Antoncik, *Phys. Rev. B* **23**, 6524 (1981).
- ¹⁷E. Antoncik, *Hyperfine Interact.* **11**, 265 (1981).
- ¹⁸J. P. Bocquet, Y. Y. Chu, O. C. Kistner, M. L. Perlman, and G. T. Emery, *Phys. Rev. Lett.* **17**, 809 (1966).
- ¹⁹G. T. Emery and M. L. Perlman, *Phys. Rev. B* **1**, 3885 (1970).
- ²⁰G. M. Rothberg, S. Guimard, and N. Benczer-Koller, *Phys. Rev. B* **1**, 136 (1970).
- ²¹H. Muramatsu, T. Miura, H. Nokahara, M. Fujioka, and E. Tanaka, *Hyperfine Interact.* **20**, 305 (1984).
- ²²D. E. Ellis, *Int. J. Quantum Chem.* **S2**, 35 (1968); D. E. Ellis and G. S. Painter, *Phys. Rev. B* **2**, 2887 (1970).
- ²³A. Rosén, D. E. Ellis, H. Adachi, and F. W. Averill, *J. Chem. Phys.* **85**, 3629 (1976).
- ²⁴D. Guenzburger, in *Local Density Approximations in Quantum Chemistry and Solid State Physics*, edited by J. P. Dahl and J. Avery (Plenum, New York, 1984), p. 573.
- ²⁵D. Guenzburger and D. E. Ellis, *Phys. Rev. B* **22**, 4203 (1980); D. Guenzburger, D. E. Ellis, P. A. Montano, G. K. Shenoy, S. K. Malik, D. G. Hinks, P. Vaishnav, and C. W. Kimball, *ibid.* **32**, 4398 (1985).
- ²⁶D. Guenzburger and D. E. Ellis, *Phys. Rev. B* **31**, 93 (1985); D. E. Ellis and D. Guenzburger, *ibid.* **31**, 1514 (1985).
- ²⁷W. Winkler, R. Vetter, and E. Hartmann, *Chem. Phys.* **114**, 347 (1987).
- ²⁸M. Grodzicki, V. Männing, A. X. Trautwein, and J. M. Friedt, *J. Phys. B* **20**, 5595 (1987); V. Männing and M. Grodzicki, *Theor. Chim. Acta* **70**, 189 (1986).
- ²⁹A. Svane and E. Antoncik, *Phys. Rev. B* **34**, 1944 (1986).
- ³⁰L. Chow, P. A. Deane, J. N. Farrell, P. A. Magill, and L. D. Roberts, *Phys. Rev. B* **33**, 3039 (1986).
- ³¹A. H. Stroud, *Approximate Calculation of Multiple Integrals* (Prentice-Hall, Englewood Cliffs, N.J., 1971).
- ³²J. C. Slater, *The Self-Consistent Field for Molecules and Solids*, Vol. 4 of *Quantum Theory of Molecules and Solids* (McGraw-Hill, New York, 1974).
- ³³W. Kohn and L. J. Sham, *Phys. Rev.* **140**, A1133 (1965); R. Gaspar, *Acta Phys. Acad. Sci. Hung.* **3**, 263 (1954).
- ³⁴Von. P. Brand and H. Sackmann, *Z. Anorg. Allg. Chem.* **321**, 262 (1963).
- ³⁵F. Meller and I. Fankuchen, *Acta Crystallogr.* **8**, 343 (1955).
- ³⁶A. Schichl, F. J. Litterst, H. Micklitz, J. P. Devort, and J. M. Friedt, *Chem. Phys.* **20**, 371 (1970).
- ³⁷A. F. Wells, *Structural Inorganic Chemistry* (Clarendon, Oxford, 1984), p. 425.
- ³⁸N. N. Greenwood and T. C. Gibb, *Mössbauer Spectroscopy* (Chapman and Hall, London, 1971), p. 390.
- ³⁹J. V. Mallow, A. J. Freeman and J. P. Desclaux, *Phys. Rev. B* **13**, 1884 (1976).
- ⁴⁰N. C. Amaral, B. Maffeo, and D. Guenzburger, *Phys. Status Solidi B* **117**, 141 (1983).
- ⁴¹M. L. de Siqueira, S. Larsson, and J. W. D. Connolly, *J. Phys. Chem. Solids* **36**, 1419 (1975).